KSME International Journal, Vol. 17 No. 1, pp. 85~96, 2003

Chaotic Responses of Curved Plate under Sinusoidal Loading

W. Y. Poon, C. F. Ng*

Department of Civil and Structural Engineering, The Hong Kong Polytechnic University, Hung Hom, Kowloon, Hong Kong SAR

Y. Y. LEE

Department of Building Construction, The City University of Hong Kong, Kowloon, Hong Kong SAR

In the present investigation, the nonlinear dynamic buckling of a curved plate subjected to sinusoidal loading is examined. By the theoretical analyses, a highly nonlinear snap-through motion of a clamped-free-clamped-free plate and its effect on the overall vibration response are investigated. The problem is reduced to that of a single degree of freedom system with the Rayleigh-Ritz procedure. The resulting nonlinear governing equation is solved using Runge-Kutta (RK-4) numerical integration method. The snap-through boundaries, which vary with different damping coefficient and linear circular frequency of the flat plate are studied and given in terms of force and displacement. The relationships between static and dynamic responses at the start of a snap-through motion are also predicted. The analysis brings out various characteristic features of the phenomenon, i.e. 1) small oscillation about the buckled position-softening spring type motion, 2) chaotic motion of intermittent snap-through, and 3) large oscillation of continuous snap-through motion crossing the two buckled positions-hardening spring type. The responses of buckled plate were found to be greatly affected by the snap-through motion. Therefore, better understanding of the snap-through motion is needed to predict the full dynamic response of a curved plate.

Key Words : Chaotic Response, Sinusoidal Loading

1. Introduction

Structural components made of curved plate elements often find applications in construction of roof and aircraft structures. Curved plate structure design is often used instead of flat plate structure design because of higher transverse stiffness, less aerodynamic resistance and better architectural appearance. However, the curved plates are generally thin due to the difficulties of manufacturing thick curved panel and the light-weight design purpose, thus they are susceptible to static and dynamic instability of snap-through motion when subject to combined in-plane and transverse loading.

Snap-through motion may cause a plate repeatedly curving inward and outward to induce large in-plane stresses, and finally lead to structural failures. In engineering practice, the design of structures against snap-through is based on the static analysis and the use of approximate correction factor to account for dynamic effects. Such simplification may result in inaccurate predictions of fatigue life, structural failure stresses, and dynamic responses. Thus, there is a need to develop an effective method of structural dynamic response analysis, coupled with accurate characterization of snap-through motion.

The static in-plane loading can be caused by mechanical or thermal stresses from the support frames. These stresses may not be present during

* **E-mail** : cecfng@polyu.edu.hk
Department of Civil and Structural Engineering, The Hong Kong Polytechnic University, Hung Hom, Kowloon, Hong Kong SAR (Manuscript **Received** May 7, 2002; **Revised** October 23, 2002)

the installation of the structure and therefore not considered in the design calculations. However the in-plane stresses can induce transverse buckling and the buckled plate will undergo snap-through instability similar to those found in arches under transverse loading. The transverse loading is generally dynamic or transient in practice and may be due to wind, airflow forced by fans, acoustic waves or impact of objects. A number of structural failures, vibration fatigue and noise transmission problems in building roof panels, aircraft fuselage and ventilation ducts were found to be caused by the dynamic snap-through motion under combined in-plane and transverse loading.

Nonlinear vibrations of a buckled beam has received significant attention in the literature and has been studied by Tseng and Dugundji (Tseng and Dugundji, 1970) whereas the studies related to chaotic responses were undertaken by many investigators (Afaneh and Ibrahim, 1992; Ji and Hansen, 2000; Brunsden et al., 1989; Pezeshki and Dowell, 1987). All these works were based on the harmonic excitation. Furthermore, Tseng and Dugundji (Tseng and Dugundji, 1970) experimentally investigated the non-linear response and large-amplitude vibration of a buckled beam with fixed ends. Later, experimental investigations of chaotic responses were reported by Tang and Dowell, Murphy and Virgin, Kreider and Nayfeh, etc (Tang and Dowell, 1988; Yamaki et al., 1981; Murphy et al., 1996; Kreider and Nayfeh, 1988; Leatherwood et al., 1992; Wolfe et al., 1995). However, the snap-through motion was not studied. A Rayleigh-Ritz analysis based on a single mode model to represent the transverse displacement of a plate due to in-plane stresses was developed by Ng (Ng, 1989a; 2000; 1996; 1989b; Poon, 2002). The response of the system under various excitations showed amplitude modulations as well as snap-through motions.

It is noted that most previous theoretical and experimental works on snap-through motion were mainly on buckled beams. This formulation in this paper is useful for two-dimensional analysis of plates subject to a uniaxial static load a transverse harmonic support motion. In this paper, a detailed parametric study to highlight the critical parameters is carried out considering a simply supported plate subject to a sinusoidal excitation using a single mode representation of displacement patterns. The intent of the paper is to develop a general understanding of the phenomena that may be applied to many engineering problems that fall in this category.

2. Formulation

2.1 Single-mode formula for a plate under compression

The starting point is the von Karman equations for large deflection of plates. Consider a free-clamped-free-clamped rectangular plate of width a in x direction and length b in y direction with thickness t acted on by a transverse pressure h. The plate is subject to horizontal displacement U in x direction. The end moves only during initial compression process and fixed for dynamic loading. The system under investigation is shown schematically in Fig. 1. The transverse equilibrium equation and the in-plane compatibility equation can be expressed, respectively, as

$$D\nabla^4 w = h + t\left(\sigma_x \frac{\partial w^2}{\partial x^2} + \sigma_y \frac{\partial^2 w}{\partial y^2} + 2\tau_{xy} \frac{\partial^2 w}{\partial x \partial y}\right) \quad (1)$$

and

$$\frac{1}{Et}\nabla^4 F = \left(\frac{\partial^2 w}{\partial x \partial y}\right)^2 - \frac{\partial^2 w}{\partial x^2}\frac{\partial^2 w}{\partial y^2} \quad (2)$$

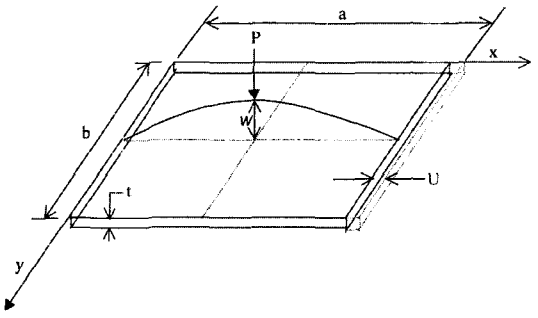

Fig. 1 Schematic diagram of a C-F-C-F plate model

where $\sigma_x=\frac{\partial^2 F}{\partial y^2}$, $\sigma_y=\frac{\partial^2 F}{\partial x^2}$, $\tau_{xy}=-\frac{\partial^2 F}{\partial x \partial y}$; F=a stress function $F(x, y)$; σ_x, σ_y, τ_{xy}=in-plane stresses; w=transverse displacement; D=plate flexural stiffness=$\frac{Et^2}{12(1-\nu^2)}$; E=modulus of elasticity; t=plate thickness; h=transverse load per unit area (pressure); ∇^4=biharmonic operator; ν=Poisson's ratio.

The steps are the same as in the Rayleigh-Ritz method and summarized as follows:

Transverse Displacement is given by

$$w(x, y)=tQ\phi(x)\psi(y) \tag{3}$$

where $w(x, y)$ =transverse displacement
tQ =modal displacement
$\phi(x)\psi(y)$=buckling mode shape function
Q =modal displacement coefficient

The corresponding modal force coefficient, P, is

$$P=t\int_0^b\int_0^a h(x, y)\phi(x)\psi(y)\,dxdy$$

where $h(x, y)$ is the transverse pressure. a and b are width and length of the plate in x and y directions, respectively.

Stress Function is given by substituting w from (3) into (2),

$$F(x, y)=F_c(x, y)+F_p(x, y)$$

where $F_p(x, y)$ is the stress function due to the shortening of the edges and $F_c(x, y)$ is the stress function due to large transverse displacement.

$$F=Et^2Q^2\sum_i\sum_j f_{ij}\phi_i(x)\psi_j(y) -\frac{1}{2}P_x y^2-\frac{1}{2}P_y x^2 \tag{4}$$

where $\phi_i(x)\psi_j(y)$ are higher order functions related to $\phi(x)\psi(y)$, respectively. f_{ij} depends on i, j (details in Ng(1989)); P_x, and P_y are mean compressive stresses in x and y directions.

Mean Compressive Stresses is given by for the edge displacement in x direction,

$$U=\int_0^a\frac{\partial u}{\partial x}dx=\int_0^a\left[\frac{\sigma_x-\nu\sigma_y}{E}-\frac{1}{2}\left(\frac{\partial w}{\partial x}\right)^2\right]dx =\int_0^a\left[\frac{1}{Et}\left(\frac{\partial^2 F}{\partial y^2}-\nu\frac{\partial^2 F}{\partial x^2}\right)-\frac{1}{2}\left(\frac{\partial w}{\partial x}\right)^2\right]dx \tag{5}$$

Substituting (3) and (4) into (5), P_x, and P_y can be derived.

For sides fixed in-plane direction $V=0$ (edge displacement in y direction being zero).

$$P_x=P_u-\frac{E}{(1-\nu^2)}C_{xy}Q^2 \tag{6}$$

$$P_y=\nu P_x-EC_yQ^2 \tag{7}$$

where $P_u=\frac{E}{1-\nu^2}\left(\frac{U}{a}\right)$.

P_u is the mean compressive stress due to edge shortening if the plate is flat and C_{xy} is a constant related to $\phi(x)\psi(y)$. C_y is a constant related to $\psi(y)$.

For sides free to move in the in-plane direction,

$$P_y=0$$

and

$$P_x=P_u-EC_xQ^2$$

where C_x is a constant related to $\phi(x)$.

In-plane Strain Energy is given by

$$V_e=\int_0^b\int_0^a\frac{t}{2E}[\sigma_x^2+\sigma_y^2-2\nu\sigma_x\sigma_y+2(1+\nu)\tau_{xy}^2]dxdy =\int_0^b\int_0^a\frac{t}{2E}\left[(\nabla^2F)^2-2(1+\nu)\left[\frac{\partial^2F}{\partial x^2}\frac{\partial^2F}{\partial x\partial y}-\left(\frac{\partial^2F}{\partial x\partial y}\right)^2\right]\right]dxdy \tag{8}$$

Substituting (4) into (8), V_e is composed of two parts, V_{ep}, the compressive strain energy due to shortening of the edges, and V_{ec}, the tensile strain energy due to the large transverse displacement.

$$V_{ep}=\frac{tab}{2E}[P_x^2+P_y^2-2\nu P_xP_y]$$
$$V_{ec}=\frac{Et^5\pi^4}{a^3}ebQ^4 \tag{9}$$
$$V_e=V_{ep}+V_{ec}$$

where e is a constant related to f_{ij}.

Bending Strain Energy is given by

$$V_b=\frac{D}{2}\int_0^b\int_0^a\left[\frac{\partial^2 w}{\partial x^2}+\frac{\partial^2 w}{\partial x^2}\right]^2 dxdy \tag{10}$$

Substituting (3) into (10)

$$V_b=Dt^2ab\frac{\pi^4}{a^4}Q^2d \tag{11}$$

where d is a constant related to $\phi(x)\,\psi(y)$.

Formulation of Static Equilibrium Equation is given by substituting (9) and (11) into the equation

$$\frac{\partial(V_{ec}+V_{ep}+V_b)}{\partial Q}=P \tag{12}$$

Linear Static Equilibrium Equation can be expressed by

$$\frac{\partial V_b}{\partial Q}=P$$

This equation applies for a flat plate with small value of Q, for which V_e can be neglected.

Substituting (11) into the above equation,

$$2Dt^2ab\frac{\pi^4}{a^4}Qd=P$$

Defining $K=2Ddt^2ab\frac{\pi^4}{a^4}$, the linear modal equilibrium equation is given by

$$KQ=P \tag{13}$$

K is thus the linear modal stiffness.

Nonlinear Static Equilibrium Equation can be obtained by substituting (9) and (10) into (12) and rearranging

$$Q\left[\left(2e+\left(\frac{C_{xy}}{1-\nu^2}\right)+C_y^2\right)\frac{Et^2\pi^2C_{xy}}{a^2}Q^2 - P_u+\frac{Dd\pi^2}{ta^2C_{xy}}\right]\frac{2t^3b\pi^2}{a}C_{xy}=P \tag{14}$$

By putting $\frac{Dd\pi^2}{ta^2C_{xy}}=P_c$, $P_c\frac{2t^3b\pi^2C_{xy}}{a}=K$

where K is the linear modal stiffness from (13)

and $Q_p^2=\dfrac{P_c}{\left(2e+\dfrac{C_{xy}}{(1-\nu^2)}+C_y^2\right)\dfrac{Et^4\pi^4C_{xy}}{a^2}}$

the equation becomes

$$Q\left[\frac{Q^2}{Q_p^2}-\left(\frac{P_u}{P_c}-1\right)\right]K=P \tag{15}$$

This is the nonlinear modal equilibrium equation. $\frac{Q^2}{Q_p^2}$ is the effect of large displacement, $\frac{P_u}{P_c}$ is the effect of compression.

Defining $\frac{E}{(1-\nu^2)}\frac{U_c}{a}$, and $\frac{P_u}{P_c}=\frac{U}{U_c}$,

and putting $q=\frac{Q}{Q_p}$ and $p=\frac{P}{KQ_p}$,

the general non-dimensional equation is obtained by dividing (15) by KQ_p.

$$q^3-(U/U_c-1)\,q=p \tag{16}$$

Putting $p=0$ for loading with in-plane compression only,

for $\frac{P_u}{P_c}<1$, $\frac{U}{U_c}<1$, , $q=Q=0$

and for $\frac{P_u}{P_c}>1$, $\frac{U}{U_c}>1$, $\frac{Q^2}{Q_p^2}=\left(\frac{P_u}{P_c}-1\right)$

$$q^2=\left(\frac{U}{C_c}-1\right)$$

From the above it can be seen that P_c and U_c are the critical mean compressive stresses and edge shortening respectively, thus when $\frac{U}{U_c}=2$,

$$Q=Q_p \text{ and } q=1 \tag{19}$$

The Kinetic Energy can be expressed as

$$V_T=\frac{1}{2}\rho t\int_0^b\int_0^a\dot{w}^2dxdy \tag{20}$$

where ρ is the density of the plate substituting (3) into (20)

$$V_T=\frac{1}{2}M\dot{Q}^2 \tag{21}$$

where $M=\rho t^3\int_0^b\int_0^a\phi^2(x)\,\psi^2(y)\,dxdy$ and M is the modal mass.

Lagrangian Equation for Linear Vibration is given by

$$\frac{\partial V_b}{\partial Q}+\frac{d}{dt}\frac{\partial V_T}{\partial \dot{Q}}=P \tag{22}$$

Using results from (12), (20), the equation of motion is obtained

$$KQ+M\ddot{Q}=P \tag{23}$$

The natural linear circular frequency of the flat configuration is thus given by

$$\Omega^2=\frac{K}{M} \tag{24}$$

The modal mass M can be written is terms of Ω

$$M=\frac{K}{\Omega^2} \tag{25}$$

Lagrangian Equation for Nonlinear Vibration is given by

$$\frac{\partial(V_b+V_{ec}+V_{ep})}{\partial Q}+\frac{d}{dt}\frac{\partial V_T}{\partial \dot{Q}}=P \tag{26}$$

Using results from (15) and (23) the modal equation of motion is obtained,

$$\left[\frac{Q^2}{Q_p{}^2}-\frac{P_u}{P_c}-1\right]KQ+M\ddot{Q}=P \tag{27}$$

Dividing both sides by KQ_p and using results from (16) and (25), the nondimensional equation of motion is obtained,

$$q^3-Rq+\frac{1}{\Omega^2}\ddot{q}=P \tag{28}$$

where $q=\frac{Q}{Q_p}$=nondimensional displacement parameter; Q=modal displacement coefficient; Q_p= value of Q at $R=1$; $R=\lambda-1$; $\lambda=\frac{U}{U_c}$; U=in-plane edge shortening displacement; U_c=value of U at which buckling starts.

The damping effect can be similarly included by dividing the modal damping force $2M\lambda\Omega\dot{Q}$ (λ is the modal damping coefficient) by KQ_p, which gives $\frac{2\xi}{\Omega}\dot{q}$. Thus the nondimensional equation of motion can be written as

$$\frac{\ddot{q}}{\Omega^2}+\frac{2\xi\dot{q}}{\Omega}+q^3-Rq=p \tag{29}$$

Nondimensional Equation: Using the von Karman equation for nonlinear analysis and the Lagrangian equation for the formulation, the following modal equations were obtained for a plate with modal displacement Q under modal force P (the equilibrium equation in the transverse direction).

For static equilibrium,

$$q^3-Rq=p \tag{30}$$

For dynamic motion,

$$\frac{\ddot{q}}{\Omega^2}+\frac{2\xi\dot{q}}{\Omega}+(q^3-Rq)=p \tag{31}$$

where Ω=linear natural circular frequency of the flat configuration; ξ=modal damping coefficient; $p=\frac{P}{KQ_p}$=nondimensional force parameter; P=applied modal force; K=linear modal stiffness of the flat plate.

The parameter Q_p, U_c, Ω, ξ, K depend on the assumed shape function of the mode and other plate parameters. The non-dimensional parameters, q, R, p, can be evaluated after Q_p, U_c, K and Ω are found by experiments or theories. The Eq. (30) involves only non-dimensional parameters and is therefore independent of the plate parameters. Actually it can be used for other boundary conditions. The finite Eq. (31) are the same for any boundary conditions although the parameters Q_p, U_c, K and Ω are changed. Using equations (30) and (31), the nonlinear static and dynamic behaviors of a plate can be predicted and they are applicable to plates of any size, boundary conditions, and material properties.

3. Prediction of Region of Chaotic Motion

This paper considers the case when there are two equilibrium positions that are not affected by the initial imperfection. The preceding formulas (30) and (31) are applicable to any plate with arbitrary boundary conditions if there is no coupling between the various modes. From formula (30), the stability relationship between p and q is known. Static equilibrium position q_o

under different R are found by putting $p=0$ in Eq. (30). For post-buckling region $R>0$, there are three equilibrium values of $\sqrt{R}$, $-\sqrt{R}$ and zero. Zero is an unstable position as the stiffness is negative.

For simplicity and easy of explanation, the free vibration differential Eq. of (31), with $p=0$ and $\xi=0$, becomes

$$\frac{\ddot{q}_1}{\Omega_2}-R_1q_1+q_1^3=0 \tag{32}$$

Since $\ddot{q}_1=\frac{d\dot{q}_1}{dt}=\frac{d\dot{q}_1}{dq_1}\cdot\frac{dq_1}{dt}=\dot{q}_1\frac{d\dot{q}_1}{dq_1}$

$$q_1=\frac{1}{2}\frac{d(\dot{q}_1^2)}{dq_1} \tag{33}$$

Substituting (33) into (32) and the resulting first order differential equation is

$$\begin{aligned}&\frac{1}{2\Omega^2}\frac{d\dot{q}_1^2}{dq_1}=R_1q_1-q_1^3\\&\frac{1}{2\Omega^2}\int d\dot{q}_1^2=\int(R_1q_1-q^3)\,dq_1\\&\frac{1}{2\Omega^2}\dot{q}_1^2=\frac{R_1q_1^2}{2}-\frac{q_1^4}{4}+c\end{aligned} \tag{34}$$

The left-hand side of Eq. (34) represents the kinetic energy and the right-hand side represents the potential energy.

Let q_{1m}, q_{10} and q_{1n} be the maximum initial displacement, static equilibrium point and minimum displacement respectively. The mid-point of the beam is displaced by a distance from q_{10} to q_{1m} and released from rest.

The initial equilibrium point is obtained by

$$\begin{aligned}&-R_1q_{10}+q_{10}^3=0\\&q_{10}^2=R_1\end{aligned} \tag{35}$$

As at the position q_{1m}, $\dot{q}_1=0$, which give

$$c=\frac{-R_1q_{1m}^2}{2}+\frac{q_{1m}^4}{4} \tag{36}$$

By the substitution of Eq. (35) and (36) into (34), the following equation is obtained:

$$\frac{1}{2\Omega^2}\dot{q}_1^2=\frac{1}{4}(q_1^2-q_{1m}^2)\,(2q_{10}^2-q_1^2-q_{1m}^2) \tag{37}$$

The maximum and minimum displacements of the vibration can be easily obtained from equation (37) by setting $\dot{q}_1=0$.

$$q_{in}^2-q_{im}^2=0\Rightarrow q_{in}=\pm q_{im}$$

or

$$2q_{10}^2-q_{1n}^2-q_{im}^2=0\Rightarrow q_{in}=\pm\sqrt{2q_{10}^2-q_{1m}^2}$$

For the case of small amplitude of vibration $q_{1m}<\sqrt{2}\,q_{10}$ (Case 1), there is no snap-through motion.

$$q_{in}=\sqrt{2q_{10}^2-q_{1m}^2} \tag{38}$$

For the case of $q_{1m}=\sqrt{2}\,q_{10}$ (Case 2), this is the limiting point of snap-through:

$$q_{in}=0 \tag{39}$$

For $q_{1m}>\sqrt{2}\,q_{10}$ (Case 3), snap-through motion will take place.

$$q_{in}=-q_{nm} \tag{40}$$

If $R1=1$, $q_{10}=1$, and then

$$q_{1m}=1.404 \tag{41}$$

Equation (37) can be modified into the following form:

$$\dot{q}_1^2-R_1\Omega^2q_1^2+\frac{\Omega^2}{2}q_1^4=\frac{\Omega^2}{2}\left[\frac{q_{10}^2q_{1m}^2}{2}+\frac{q_{1m}^2}{4}\right] \tag{42}$$

Substituting (41) into (42), $R_1=1$ yields

$$\dot{q}_1^2-\Omega^2q_1^2+\frac{\Omega^2}{2}q_1^4=\frac{3\Omega^2}{4} \tag{43}$$

Equation (43) is plotted in Fig. 2 in nondimenisonalized form for various values of q_{1m}. There are three static equilibrium positions, one unstable in the origin and two stable positions elsewhere. Note that the trajectories depart from a circular shape when the amplitude q_{1m} grows. The motion taking place in the two domains centered about the two stable equilibrium positions varied with the buckling parameter R_1. The state plane at the critical boundary for different buckling parameter R_1 is shown in Fig. 3. It can be seen that the two centers are square root of the buckling parameter R_1.

In this section, results of the numerical integration will be presented for a curved plate with R= 1 subject to a sinusoidal force. For $R<1$, snap-through motion will not inpractice exist because the initial buckling displacement is too small. The Runge-Kutta (RK-4) technique is adopted to analyze the equation of motion of a buckled plate

(31) with $\xi=0.01$, $\Omega=63$ rad/s, $q_o=1$, $p=p_o \sin \omega t$, where p_o and ω are the amplitude and circular frequency of the excitation force, respectively. The linear natural circular frequency of the buckled plate is $\Omega\sqrt{2}=89.1$ rad/s.

First, the non-dimensional force amplitude p_o varies from 0.05 to 4 and the vibration responses in terms of mean displacement and R.M.S. displacement are found for various forcing frequencies. The results are presented in the form of the non-linear responses q of the curved plate versus the circular frequency ω. Depending on the force amplitude p_o, Figs. 4 to 9 yield three regions of distinct non-linear dynamic behaviour comprising softening spring, chaotic and hardening spring. The chaotic type of vibration or snap-through motion appears due to an instability condition. The dynamic instability regions for the single mode response of a buckled plate under sinusoidal load are presented in Table 1.

It is shown in Figs. 4 to 9 that the R.M.S. amplitude of the response increases with the excitation force p_o. As for a constant magnitude of p_o (say $p_o=0.05$), the amplitude of vibration q_{rms}

Table 1 Dynamic instability region for single mode response

Displacement or Strain Response	No Snap-through Region	Intermittent Snap-through Region	Continuous Snap-through Region
Mean $q(mean)$	Static value	Unsteady	Zero
R.M.S. $q(rms)$	<20%static value	Jump with Excitation	>70% of static value
Non-linearity	Softening	Unstable	Hardening

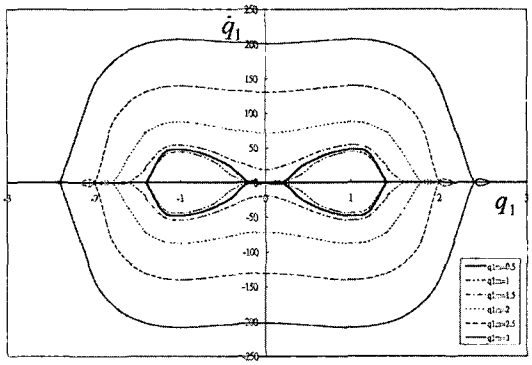

Fig. 2 State plane for different initial displacements q_{1m} with $R_1=1$

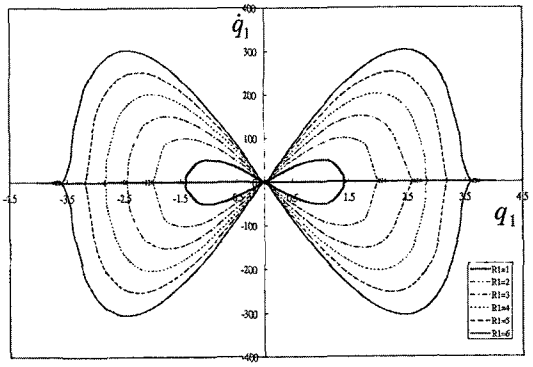

Fig. 3 State plane at critical boundary for several values of q_{10} ($q_{10}^2=R_1$)

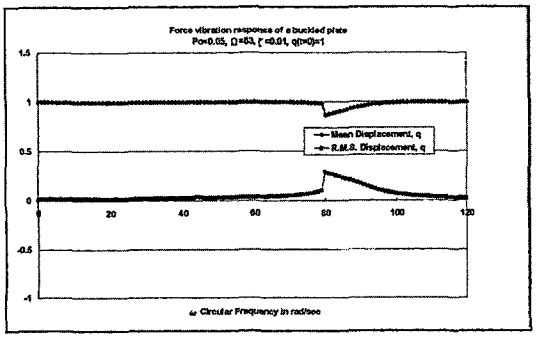

Fig. 4 Plot for soft sping behavior at 80 rad/s with $p_o=0.05$

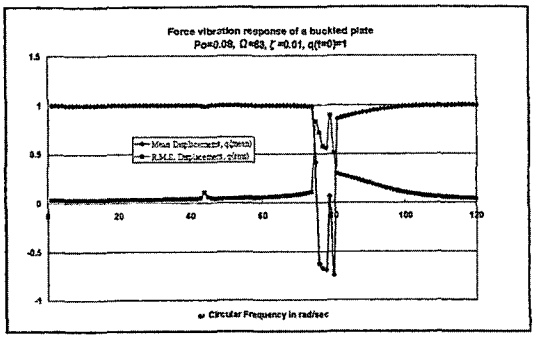

Fig. 5 Plot for chaotic behavior at 74 to 81 rad/s with $p_o=0.08$

exhibits a peak phenomenon when the excitation frequency ω is slowly increased. Similarly, the q_{mean} value causes a trough at the same frequency. It is evident in Fig. 4 that the softening spring behaviour appears before the initiation of the snap-through motion.

The chaotic behavior is found to begin when p_o exceeds 0.065 with $q_{rms}=0.422$. It is shown in Fig. 5 that the snap-through motion occurs when amplitude of force p_o equals 0.08. Chaos is the instability behavior of a system. The movements of q_{rms} and q_{mean} are irregular, non-periodic and intermittent. When the amplitude of the excitation force p_o is increased from 0.08 to 0.35, the region of circular frequency ω that causes chaotic vibration response becomes wider. At $p_o=0.35$,

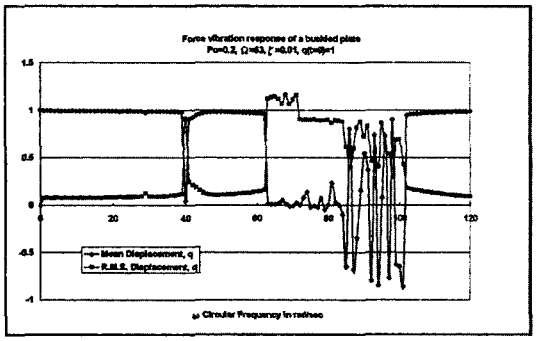

Fig. 6 Plot for chaotic behavior with $p_o=0.2$

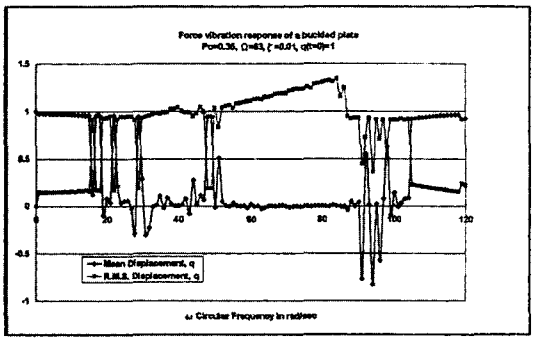

Fig. 7 Plot for chaotic behavior with $p_o=0.35$

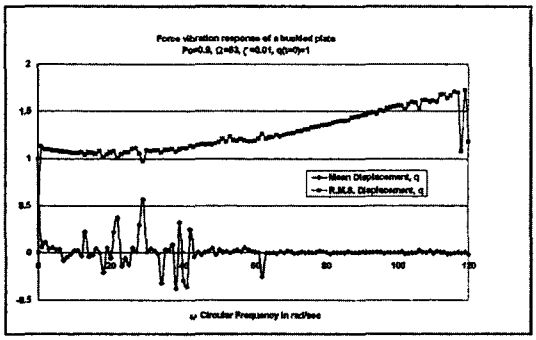

Fig. 8 Plot for hardening spring effect with $p_o=0.9$

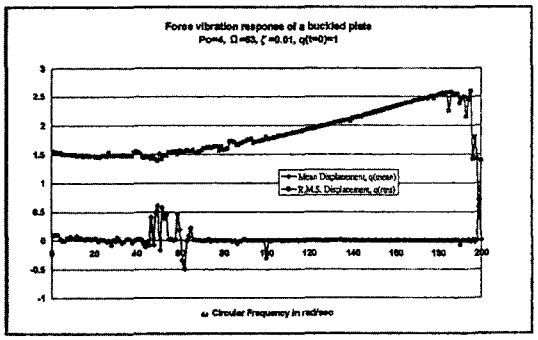

Fig. 9 Plot for hardening spring effect at $p_o=4$

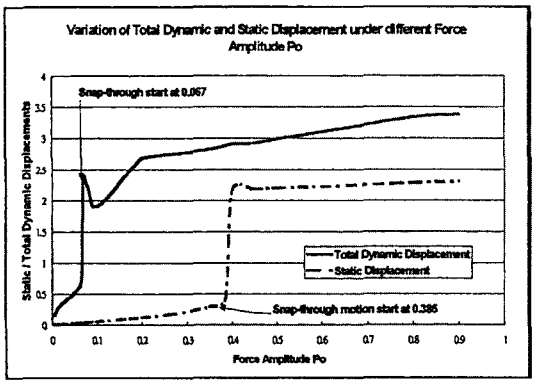

Fig. 10 Plot for maximum $q(rms)$ with $p_o=0.05$ to 0.9

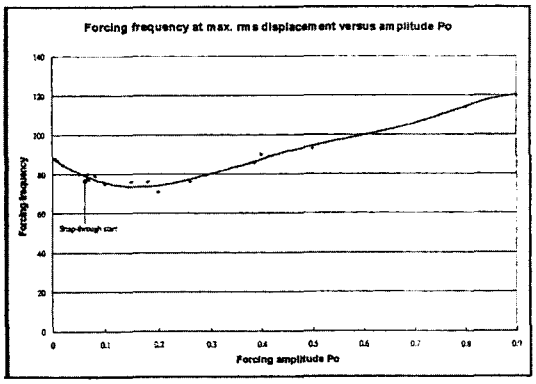

Fig. 11 Plot for ω at max. $q(rms)$ with p_o

unsteady snap-through motions starts at $\omega=16$ rad/s and ends at $\omega=107$ rad/s. Under the instability conditions, the snap-through (chaotic) motion occurs as indicated by $q_{rms}=0.9$ (close to 1.0) and $q_{mean}=0.07$ (close to zero). The q_{rms} value for the steady and continuous snap-through region rises up to a peak response of 1.3. It is observed that subharmonic resonances that play an important role in pre-chaotic vibration occurs at various frequencies such as 18 rad/s, 28 rad/s, 40 rad/s & 48 rad/s.

When p_o is increased to 0.9, steady and continuous snap-through motion occurs up to $\omega=120$ rad/s as indicated by Fig. 8 where $q_{mean}=0$. The q_{mean} is equal to zero because the snap-through motions are continuous. A jump phenomenon occurs at $\omega=120$ rad/s, indicating the hardening spring resonance. It should be noted that flat plates without the snap-through motion show the hardening spring effect only. Figure 9 shows the response curve shifting upward to $q=1.5$ when p_o is equal to 4. The response continues to increase with p_o until the material failure occurs.

It is shown in Fig. 10 that the total dynamic displacement changes rapidly when $p_o=0.067$. The irregular pattern between $p_o=0.067$ and $p_o=0.2$ exhibits the non-periodic response and it demonstrates the transition zone between the softening spring and hardening spring effects. The nondimensional displacement rises up constantly after p_o equal 0.2. It is clear that the static displacement value in Fig. 10 loses its stability at 0.385. The ratio of the force amplitude between the static and dynamic motion at the bifurcation point (onset of snap-through) is 5.75. Figure 11 indicates that the forcing frequency of maximum q_{rms} comes to a minimum point at $\omega=75$ rad/s when the forcing amplitude increases. An interesting observation here is that the maximum displacement has a tendency to expand to a lower frequency first with softening spring behaviour and then goes up to a higher frequency with hardening spring effect. The lowest region exhibits the chaotic nonlinear behaviour.

4. Analysis of Results

Since the nondimensional force parameters depend upon the modal damping coefficient ξ and the linear circular frequency of the flat plate Ω, similar results were obtained for different Ω (related to mass) and ξ (related to damping). The relationships between various parameters are tabulated in Tables 2 and 3.

Table 2 Comparison of the static and dynamic instability region for different ξ

Instability Region begins at (Fixed $\Omega=63$)	Static	Dynamic $\xi=0.01$	Dynamic $\xi=0.03$	Dynamic $\xi=0.05$	Dynamic $\xi=0.07$	Dynamic $\xi=0.1$	Dynamic $\xi=0.7$
Nondimensional Force Parameter p_o	0.385	0.065	0.085	0.11	0.145	0.178	0.3
Nondimensional Displacement Parameter $q_{rms}(q_o=1)$	0.423	0.422	0.403	0.350	0.452	0.383	0.412

Table 3 Comparison of the static and dynamic instability region for different Ω

Instability Region begins at (Fixed $\xi=0.01$)	Static	Dynamic $\Omega=8$	Dynamic $\Omega=16$	Dynamic $\Omega=31.5$	Dynamic $\Omega=63$	Dynamic $\Omega=80$	Dynamic $\Omega=100$
Nondimensional force parameter p_o	0.385	0.067	0.063	0.065	0.065	0.063	0.067
Nondimensional Displacement parameter q_{rms} at $q_o=1$	0.423	0.301	0.448	0.344	0.422	0.355	0.408

Tables 2 and 3 examine the instability regions generated by Eqs. (30) and (31) for plates with different Ω and ξ under transverse force. It is observed that the points of dynamic instability with fixed ξ are generally consistent for different Ω. It is also observed that for fixed Ω, the points of dynamic instability due to p_o show a linear relationship with ξ. It is also interesting to note that the displacement parameter q maintains a fairly constant range between 0.3 to 0.45 for the start of the snap-through motion. This can be expected since the parameter of dynamic stability is $q=0.3$ for all cases. Another parameter of dynamic stability is force parameter p_o which is expected to increase with increased modal damping coefficient ξ. Comparing the corresponding results for constant ξ and constant Ω, it is generally observed that the plate under dynamic loading has lower point of unstable region than that under static loading.

From Figs. 4 to 9, it is observed that three regions of different nonlinear dynamic behavior are presented. Different regions have their own characteristics :

1. **Softening spring** - the resonant frequency decreases with amplitude and the jump behavior occurs at the left-hand side of the resonant frequency. Dynamic displacement $\Delta q<0.3$, mean displacement $q=\sim 1$. Figure 12 shows the time history of the softening spring effect in which the plate or beam moves in a small oscillation in the neighborhood of the initial position 1.
2. **Chaotic** - the response is non-periodic, intermittent and jumps up and down around the two positions $q=1$ and -1. This is called the snap-through motion between the static equilibrium positions. The snap through motion is of very low frequency and large amplitude when compared with the oscillation around the static equilibrium position. Dynamic displacement $0.3<\Delta q<1$, mean displacement $0<q<1$. The chaotic region serves as the transition between two paths (see Fig. 13).
3. **Hardening spring** - when the snap-through motion gets more repetitions and of larger amplitude, the response becomes periodic again. In this case, the snap-through motion occurs in every cyclic of vibration. The frequency is initially low and increases rapidly with amplitude. The jump behavior is to the right hand side of the resonant frequency. Dynamic displacement $\Delta q>1$, mean displacement $q_{mean}=0$. Figure 14 shows the time history of the hardening spring behaviour.

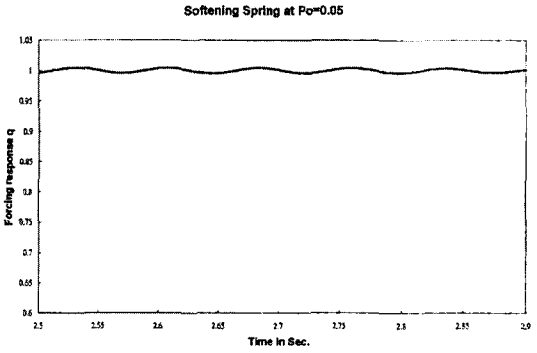

Fig. 12 Time history of softening spring behaviour

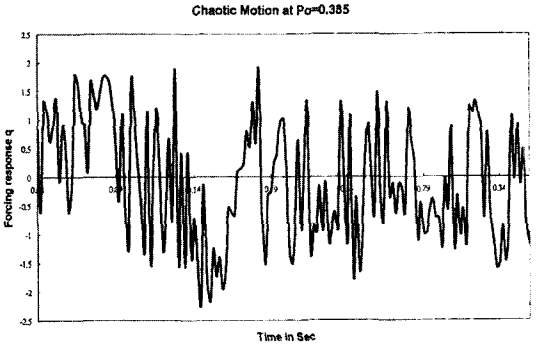

Fig. 13 Time history of chaotic motion

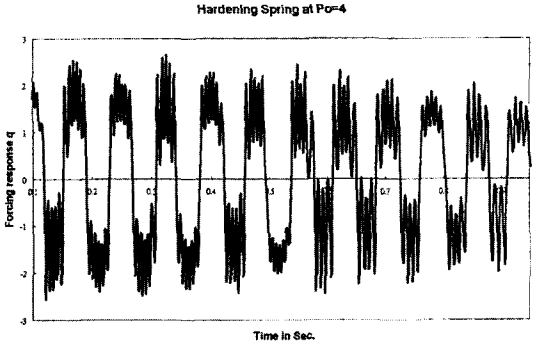

Fig. 14 Time history of hardening spring behaviour

5. Conclusions

The response of a nonlinear plate due to harmonic excitation has been investigated. The large amplitude vibration of a curved plate shows the snap-through motion due to instability. The intermittent snap-through serves as a transition region from the softening spring behavior to the hardening spring behavior. The presence of the snap-through motion requires special care in measuring the mean and r.m.s. values and frequencies of the dynamic displacement responses. Results with fixed Ω or ξ were compared with each other to investigate the behaviors of instability. From the detailed analysis, the following observations have been made:

(1) The amplitude of vibration response q_{rms} is close to the static equilibrium value at the point of initiation of the snap-through motion for all cases.

(2) For a given linear circular frequency of flat plate Ω, the force parameter p_o at the onset of snap-through motion is linearly proportional to the damping coefficient ξ.

(3) For a given damping coefficient ξ, the force parameter p_o maintains a fairly stable value with different Ω at the starting point of the snap-through motion.

(4) The present investigation has attempted to show the nonlinear vibration behaviour of buckled plate and its stability boundaries under different parameters.

(5) The prediction can provide useful information about the onset of the snap-through motion so that the plate can be designed with maximum reliability.

Acknowledgment

The present study has been sponsored by University Grant Committee (UGC) Fund no. POLYU5055/00E.

References

Afaneh, A. A. and Ibrahim, R. A., 1992, "Nonlinear Response of an Initially Buckled Beam with 1 : 1 Internal Resonance to Sinusoidal Excitation," *ASME*, DE-vol. 50/AMD-vol. 144, pp. 69~81.

Brunsden, V., Cortell, J. and Holmes, P. J., 1989, "Power Spectra of Chaotic Vibrations of a Buckled beam," *Journal of Sound and Vibration*, Vol. 130, pp. 1~25.

Ji, J. C. and Hansen, C. H., 2000, "Nonlinear Response of a Post-Buckled Beam Subjected to a Harmonic Axial Excitation," *Journal of Sound and Vibration*, Vol. 237, No. 2, pp. 303~318.

Kreider, W. and Nayfeh, A. H., 1988, "Experimental Investigation of Single-Mode Response in a Fixed-Fixed Buckled Beam," *Nonlinear Dynamics*, Vol. 15, pp. 155~177.

Leatherwood, D., Clevenson, S. and Powell, C. A., 1992, "Acoustic Testing of High-Temperature Panels," *J. Aircraft*, Vol. 29 No. 6, pp. 2632~2640.

Murphy, K. D., Virgin, L. N. and Rizzi, S. A., 1996, "Experimental Snap-Through Boundaries for Acoustically Excited, Thermally Buckled Plates," *Experimental Mechanics*, Vol. 36, pp. 312~317.

Ng, C. F., 1989, "Nonlinear and Snap-Through-Responses of Curved Panels to Intense Acoustic Excitation," *Journal of Aircraft*, Vol. 26, No. 3, pp. 281~288.

Ng, C. F., 1989, "The Analysis of Non-Linear Dynamic Behaviour (Including Snap-Through) of Post-Buckled Plates by Simple Analytical Solution," NASA Technical Report 181877.

Ng, C. F., 1996, "Testing Techniques for Chaotic Vibration of Buckled Aircraft Structures," *ImechE*, Vol. 210, pp. 281~289.

Ng, C. F., 2000, "The Nonlinear Acoustic Response of Thermally Buckled Plates," *Applied Acoustics* 59, pp. 237~251.

Pezeshki, C. and Dowell, E. H., 1987, "An Examination of Initial Condition Maps for the Sinusoidally Excited Buckled Beam Models by Duffing's Equation," *Journal of Sound and Vibration*, Vol. 117, pp. 291~232.

Poon, W. Y., 2002, "Analytical Model for Predicting Nonlinear Random and Snap-Through Response of Buckled Plates," *International Jour-*

nal of Structural Stability and Dynamics, Vol. 2, No. 1, pp. 1~24.

Tang, D. M. and Dowell, E. H., 1988, "On the Threshold Force for Chaotic Motions for Forced Buckled Beam," *ASME*, Vol. 55, pp. 190~196.

Tseng, W. Y. and Dugundji, J., 1970, "Nonlinear Vibrations of a Buckled Beam Under Harmonic Excitation," *J. Applied Mechanics*, Vol. 37, pp. 292~297.

Wolfe, H. F., Shroyer, C. A., Brown, D. L. and Simmons, L. W., 1995, "An Experimental Investigation of Nonlinear Behavior of Beams and Plates Excited to High Levels of Dynamic Response," Technical Report WL-TR-96-3057, Wright Laboratory, Wright Patterson AFB, Ohio.

Yamaki, N., Otomo, K. and Chiba, M., 1981, "Nonlinear Vibrations of Clamped Circular Plate with Initial Deflection and Initial Displacement pt. II Experiment," *J. Sound and Vibration*, Vol. 79, No. 1, pp. 43~59.